Probing topological phase transitions with string-net models and their tensor network representations

Yin Hei Chow

Supervisor: Prof. Chenjie Wang

Research project submitted as part of PHYS3999, The University of Hong Kong

April 24, 2025

Abstract

Exact diagonalization was first done on Fibonacci string-net condensate perturbed with string-tension on a small system size [1]. A tensor network method [2] combining two previous ideas [3, 4] was later used to attain a contradicting result on the nature of phase transition point. More specifically, the tensor network ansatz on the infinite lattice predicts a second order transition at where the earlier work predicted a first order transition, and it is impossible to judge whether one of negligible finite-size effect and the exapolation of the one-side tensor network ansatz through a non-analyticity is more justifiable than the other. This is because the first-order tensor network ansatz is not implemented in the abovementioned work, and one-side of the quasi-adiabatic continuation operator is omitted without justification. This work attempts to improve on the method, and thereby, obtain the first-order approximation across the phase transition. Apart from the Fibonacci string-net model, our proposed method can be implemented with Tambara-Yamagami category for $\mathbb{Z}_3$ string-net model, which is a larger system housing 15 non-trivial anyons. This first-order tensor network ansatz doesn't have larger computational complexity.

Contents

1 Introduction

Two problems are of interest in the study of topological phases - edge modes and topological orders. This report concerns with the latter, and in particular, the topological phase transitions from 2+1d topological order to the trivial topological order.

Topological orders in 2+1d are characterized by their anyon data in terms the modular matrices describing their topological spins (self statistics) and mutual statistics. In constrast to symmetry-protected topological phases, topologically ordered phases arise due to the presence of long-range entanglements [5]. These long-range entanglements provide topological protection to the anyons in that the anyons are robust against any local perturbations, or finite compositions of (piece-wise) local unitrary transformations to be precise [5]. The consequence is that anyonic models attract ample of attention from the field of quantum computation ever since topological protection has intimated a clear path towards realizing quantum memory and universal quantum computation that are stable against any local noises from the enironment - perform computations with anyons in a gapped system [6]. These works include simulating anyons on quantum processors [7, 8, 9] and in writing universal gate sets from anyon braiding [10, 11, 12].

What gives 2+1d topological orders their tremendous applicability is precisely what makes their study extremely difficult. Their preservations under local unitrary transformations imply that the orderred phases are invisible to any candidate local order parameters [5]. These phase transitions are beyond Landau symmetry-breaking paradigm [13], as was early observed that distinct topological orders can share the same symmetry [14].

Still, all is not lost, and the past decade has since increasing evidences that by generalizing the very notion of symmetry, topological orders can be classified by generalized symmetries that are not necessarily group-like nor local [15]. In particular, the subset of all 2+1d achiral topological orders that fits within the injective-PEPS formalism [16] are classified by virtual symmetries. So long the PEPS-map is injective, meaning there exists a left inverse from the Hilbert space back onto the virtual level, non-local string operators acting on the PEPS representation of the ground-states can be pulled back via this inverse and thereby be represented as matrix product operators (MPO) on the virtual level [16], as will be illustrated in the methodology section. More generally in any dimensions, a continuous topological phase transition with a finite (group) symmetry is associated with a categorial

symmetry, and the breaking of it determines the topological order [15].

Despite these attempts in extending a Landau symmetry-breaking paradigm to continuous topological phase transitions, not only are the generalized symmetries of topological orders difficult to be determined in general, how these symmetries on both sides of a critical point constrain, or completely determine, the scaling behaviors is largely unknown. This is analogous to the question "To what extent can a modified universal scaling hypothesis hold between a pair of broken categorical symmetries?". Numerical studies like this work is therefore needed as a first probe to the lay foundations for answering these big questions, in ways like determining whether a topological phase transition is even critical to start with.

The generalized string-net model realizes all achiral doubled topological orders in 2+1d [17], and therefore presents itself as a natural tool for studying a large subclass of topological phase transitions. To drive the ground-state out of the topological order, the charge-free generalized string-net model with string-tension (SNST) is used in this work, following the subject of [1, 4, 2] Despite the model's generality, the limit without string-tension is exactly soluble [17], and this property plays a vital role in making possible the numerical method proposed in this report.

Note that there exists other choices of perturbation to the string-net model that drives a topological phase transition, such as ones that involve letting fluxes to take on distinct energy costs [18, 19]. However, these kinds of perturbation commute with the string-net Hamiltonian, and by the fact that their Hamiltonians consist of only commuting projectors, these models can never have topological orders that persist at finite-temperature [20]. In constrast, string-tensions do not commute with the string-net Hamiltonian, and some thermal fidelity can be expected in general from the topological orders realized by SNST.

SNST with Fibonacci fusion rules is first studied using exact diagonalization to reveal a continuous topological phase transtion [1]. A mean-field approximation of SNST is then found with closed form solutions for all values of the total quantum dimension of the topological order, and in conflict with the former result, the phase transition corresponding to the Fibonacci fusion rules is determined to be discontinuous [4]. Developing upon [4], [2] modified their ground-state ansatz and solved the new ansatz numerically by resolving using the tensor network representation. The tensor network representation follow the same vein as the three-legged tensor network first devised in [21, 22] (though not explicitly referenced). The ground-state ansatz used in [2], like the mean-field approximation, is only perturbatively exact to the zeroth order, and therefore it is not surprising that a discontinuous phase transition is also obtained for Fibonacci fusion rules.

The research gap is then concerning the order of the topological phase transition of SNST with Fibonacci fusion rules. While the tensor network ansatz is done on an infinite projected-entangled-pair-state (PEPS) and thence does not suffer from the finite-size effect like exact diagonalization does [2], the result is a zeroth order approximation. This report proposes an improvement of the tensor network ansatz that includes the first order correction while having the exact same computational complexity. This is a proof-of-concept to show that, by pulling back evolution operators onto the entanglement degrees of freedom via the PEPS-map (as will be made clear in subsequent sections), first and possibly higher order corrections could be added to the tensor network ansatz following [3, 2] without increasing the computational cost.

2   Background

Topological orders in 2+1d are described by unitrary modular tension category (UMTC). For this discussion, we restrict only to those UMTC that are the Drinfeld centres of some unitrary fusion category (UFC), and it turns out this collection is equivalent to all achiral doubled topological orders in the string-net model [17].

2.1   Introduction to monoidal category

A group is a set equipped with an associative binary operation and an identity, such that each element has a (left) inverse. There are various generalizations for group, including the groupoids, used in the study of path-homotopy, and monoids. Intuitively, categories are to monoids like groupoids are to groups, and in particular, a category with only one object and with invertibility for all its morphisms forms a group.

The fusion category is a vector-enriched monoidal category, where the monoidal product (or tensor product) describes fusion. The tensor unit is therefore naturally the vaccum, in that any anyons fuse into the vacuum to give themselves. The objects in this monoidal category are all formal sums of simple objects called "string-types", and the morphisms are not relevant in describing fusion. The tensor product, denoted $\times$, is defined on the simple objects and then extended to all objects (and morphisms) by distributivity, following

$$a \times b = \sum_c N_{ab}^c c$$

for some fusion multiplicities $N_{ab}^c \in \mathbb{N}_0$. When N_{ab}^c is non-zero, c is said to be a fusion channel of a fusing with b. In this report, we restrict ourselves to UFC, meaning $N_{ab}^c \in \{0, 1\}$.

2.1.1   Associators & their coherence

Fusion is in general non-associative, and the how badly associativity is violated is measured by the associator. The associator F is a naturally isomorphism

$$F : ((\cdot) \times (\cdot)) \times (\cdot) \xmapsto{\cong} (\cdot) \times ((\cdot) \times (\cdot))$$

that is compatible with fusion $\times$. This compatibility involves two coherence relations, and is important for defining the ground-state wavefunction in the next section. The triangle relation states that
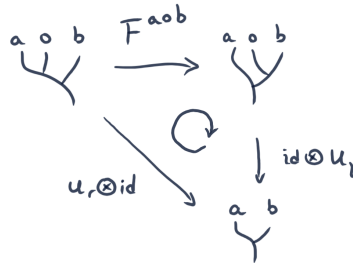
forms a commutative diagram, with u_l, u_r being the left and right unitors. Similarly, pentagon relation states that

$$F_{egl}^{fcd} F_{efk}^{abl} = \sum_h F_{gfh}^{abc} F_{egk}^{ahd} F_{khl}^{bcd}$$

where we have used the notation that F^{abc} is a component map of the natural transformation F, and that the lower indices are defined such that F^{abc}_{def} is the (e, f)-th element of the change of basis matrix from the local basis

to the new local basis

for each of the fixed d . Intuitively, the pentagon relation asserts that the diagram
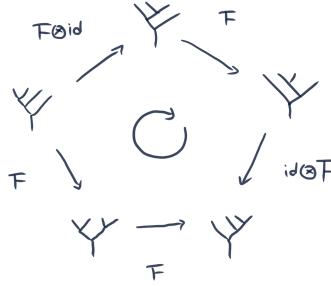
commutes, where the tree notations without indices are functors from a product category of the UFC to itself by taking tensor product in the order specified by the tree going from top to bottom. These notations will be used for defining the ground-state wavefunction of interest in subsequent sections, and as will be elucidated by then, the coherence relations are the self-consistency conditions of the ground-state wave-function.

Below, the construction of the charge-free string-net model with string-tension in this study is laid out, starting from the generalized string-net model [17].

2.2 Generalized string-net model

The generalized string-net model takes in an arbitrary unitary fusion category (UFC) and output its Drinfeld centre as the resultant 2+1d topological order.

2.2.1 Hilbert space & ground-state wavefunction

The Hilbert space has an orthonormal basis formed by all string-net configurations, and these configurations are motivated by worldlines on 1+1d. On a two-dimensional manifold, defined a time-orientation on it if possible. Then a string-net configuration, being a basis state, is a trivalent graph defined on this manifold, such that each link is labelled by a string type from the UFC, and the fusion rules of these string type are satisfied on each vertex. An extra requirement is that all these links must have no-where vanishing time-partial derivatives. Put another way, the simple objects from a UFC can be though as living on a one-dimensional space and fusing (or splitting) from each other as the virtual time progresses. Each of the possible ways for a collection of the simple objects to fuse and split in the space-time manifold is one string-net configuration, that is in turn used to define and

span our Hilbert space. In this way, trajectories of simple objects in the virtual 1+1d space-time are the links of a trivalent graph, and fusions of these objects happen at the vertices, explaining why the fusion rules are enforced on vertices. Also, these links are free to deform as long as they do not intersect each other nor have zero time-partial derivative somewhere on the path. For our discussion, the model will be defined on an open disk because the non-trivial ground-state will be unique, and the vertical direction in any diagrams hereafter will be the time-orientation.

Theorem. *Time-orientation has nothing to do with surface orientability.*

Proof. A time-orientation can be defined on both toric and Klein bottle, with the latter non-orientable. The sphere is an orientable surface but there's no consistent time-orientations that can be chosen on it due to the hairy ball theorem, which states that a continuous nowhere-vanishing vector field cannot be defined on a sphere. Yet, non-orientable surfaces, even when it is time-orientable, poses the restriction that any string-net configuration is reflectionally symmetric, and hence are not usually considered. There must exists a Mobius strip embedded in the non-orientable surface on which any diagrams can be translated into its mirror image. $\qquad\square$

Unlike most models where the Hamiltonian is defined before the ground-state is solved for, the string-net Hamiltonian is motivated and crafted to bring forth a certain ground-state. The ground-state will therefore be defined first in this introduction. Define the ground-state wavefunction as a formal sum over all string-net configurations ($s.n.$) of the surface

$$|GS\rangle = \sum_{s.n.} \psi(s.n.)|s.n.\rangle$$

where the amplitudes ψ are defined recursively using the following local relations

$$\psi\left(\overset{a\,b\,c}{\underset{e}{\bigvee}_d}\right) = \sum_f F^{abc}_{def}\,\psi\left(\overset{a\,b\,c}{\underset{d}{\bigvee}_f}\right)$$

$$\psi\left(\overset{a\quad b}{\big|\,\big|}\right) = \sum_c \frac{1}{Y^{ab}_c}\,\psi\left(\overset{a\quad b}{\underset{a\quad b}{\bigvee}_c}\right)$$

$$\psi\left({}_c\overset{a}{\underset{b}{\ominus}}{}_d\right) = \delta_{ab}\,Y^{cd}_b\,\psi\left(\big|\,a\right)$$

for all diagrams such that the fusion rules hold, and a boundary condition of

$$\psi(0) = 1$$

where 0 denote the vaccum state.

2.2.2 Elementary results on the ground-state wavefunction

Theorem. *The time-reversal $\widetilde{F}$ of associator, defined by*

$$\psi\left(\overset{e}{\underset{a\,b}{\bigwedge}}{}^d_c\right) = \sum_f \widetilde{F}^{abc}_{def}\,\psi\left(\overset{d}{\underset{a\,b\,c}{\bigwedge}}{}^f\right),$$

can be completely determined from F and Y .

Proof. Consider the following two paths of reduction

$$\left\langle \text{(diagram)} \right| = \sum_{e'} (F_d^{abc})^\dagger_{fe'} \left\langle \text{(diagram)} \right|$$

$$= (F_d^{abc})^\dagger_{fe} Y_e^{ab} Y_d^{ec} \left\langle 1_d \right| ,$$

$$\left\langle \text{(diagram)} \right| = \sum_{f'} (\widetilde{F}_d^{abc})_{ef'} \left\langle \text{(diagram)} \right|$$

$$= (\widetilde{F}_d^{abc})_{ef} Y_f^{bc} Y_d^{af} \left\langle 1_d \right|$$

Equating them gives

$$(F_d^{abc})^\dagger_{fe} Y_e^{ab} Y_d^{ec} = (\widetilde{F}_d^{abc})_{ef} Y_f^{bc} Y_d^{af} .$$

$\square$

2.2.3 Parent Hamiltonian

Notice that any trivalent graphs (with a consistence time-orientation on the links) can be embedded into a honeycomb lattice by filling in vacuum links where needed. Therefore, we will assume without loss of generality that our string-net model is on an infinite honeycomb lattice hereafter. Following [17], a Hamiltonian that give rises to the above ground-state is

$$H = -J_Q \sum_{v \in \Lambda} Q_v - J_B \sum_{p \in \Lambda^*} B_p$$

for arbitrary J_Q and J_B . Operators Q_v acts on vertex v and projects onto the states that obey the fusion rules locally. This is to say, Q_v is one if fusion rule holds locally at v and zero if the fusion rule is violated at v . Operator B_p is a projector on the nearest twelves sites around plaquette p , and is defined as

$$B_p = \sum_s \frac{(Y_0^{s\bar{s}})^*}{D^2} B_p^s$$

where the sum is over all string-types, $\bar{s}$ is the unique dual string-type of s such that the vacuum in contained in their fusion product, D is a normalization constant called total quantum dimension of the UFC, and lastly, B_p^s defined by

acts on a bra-state by inserting a loop of type s around the hole in the middle of p . Therefore, the Hamiltonian comprises of 3- and 12-site stabilizers of, and only of, the desired ground-state. In addition, all Q_v and B_p are shown to commute [17].

Theorem. *For all p, B_p is a stabilizer of the ground-state.*

Proof. The eigen-equations $B_p^s|\psi\rangle = Y_0^{s\bar{s}}|\psi\rangle$ can be derived as follows,

where the sum is over all string-net configurations (s.c.), and only plaquette p is shown in the bra- and ket-state out of the infinite number of plaquettes. Next,

$$B_p|\psi\rangle = \frac{1}{D^2}\sum_s (Y_0^{s\bar{s}})^* B_p^s|\psi\rangle = \frac{\sum_s d_s^2}{D^2}|\psi\rangle = |\psi\rangle$$

concludes the proof. As a note of caution, we have pulled one side of the s-loop over the hole in the middle of the plaquette, and this is not possible for general configurations with arbitrary string types, like those states we will encounter in the methodology section. This is due to the presence of fluxes. $\qquad\square$

2.3 Charge-free string-net model with string-tension

Since operators Q_v and B_p are local symmetries, we borrow the language of gauge theory to refer to their symmetry charges as charges and fluxes respectively. Q_v are then interpreted as gauge symmetries to be enforced, giving us a new Hilbert space as a quotient space of the original over the group action of Q_v . Put another way, we restrict ourselves to the charge-free sector by doing the follow: First, modifies the string-net Hamiltonian by adding a large constant and get

$$H = -J_Q \sum_{v \in \Lambda}(Q_v - 1) - J_B \sum_{p \in \Lambda^*} B_p$$

Next, take the limit as $J_Q \to +\infty$ to get

$$H = -J_B \sum_p B_p$$

The generalized string-net model consists only of commuting projectors, and so it can never exhibit its topological at a finite-temperature [20]. To fix this, string-tension is added to the string-net model as a non-commutative term to the flux measurement B_p . Adding in string-tension gives the model a different and unknown categorical symmetry, and increasing the string-tension beyond a certain threshold destroyes the topological order. The model Hamiltonian is

$$H = -J_B \sum_p B_p - J_l \sum_l L_l$$

where J_l is the string-tension, and L_l is a projector on the link l onto the vacuum state. That is, it acts as the identity if the string-type occupying link l is the vacuum, and zero otherwise. Below, we let $J_L = sin\theta$, $J_B = cos\theta$ to parameterized the phase transition with a single parameter $\theta \in [0, \pi/2]$, which will also be called string-tension, with a slight abuse of nomenclature.

2.4 Projected entangled-pair state

Projected entangled-pair state (PEPS) [23] extends the matrix product state (MPS) into two-dimension. It is a decomposition of the wavefunction into a tensor contraction of site tensors. The tensor network is usually taken to reflects the geometry of the underlying lattice, so the bond dimensions can be interpreted as entanglement degrees of freedom. Site tensors T_i are then linear maps from the virtual level (also called entanglement level) to the physical level, or the local Hilbert space of site i . For example, on a square lattice they read

$$T_i : (\mathbb{C}^D)^{\otimes 4} \to \mathbb{C}^d$$

where D is the bond dimension for entanglement, d is the physical dimension of the local Hilbert space, and so T_i is a rank 5 tensor. This decomposition will be heavily used in the methodology section, where we reformulate the string-net ground-state wavefunction, written in the language of fusion category, into the language of tensor networks.

3 Methodology

With the string-tension, the model is no longer soluble, and we turn to numerical schemes on the tensor network representations of perturbed ground-state wavefunction.

3.1 Ground-state ansatz & its theoretical properties

Following [3, 2], a first-order ansatz is obtained to be

$$|\alpha, \beta, \eta\rangle := \mathcal{N} \prod_l e^{\beta L_l} \prod_p e^{-\eta B_p} \prod_p (1 + \alpha Z_p)|0\rangle$$

where $Z_p = 2B_p - 1$, and α, β, η are variational parameters to be optimized for the Hamiltonian at a specific value of string-tension θ . For each value of θ , the variational parameters are determined to be

$$(\alpha^*, \beta^*, \eta^*) := \underset{\alpha\beta\eta}{\mathrm{argmin}} \frac{\langle \alpha, \beta, \eta | H(\theta) | \alpha, \beta, \eta \rangle}{\langle \alpha, \beta, \eta | \alpha, \beta, \eta \rangle}$$

The variational principle states that since the energy eigenstates form a basis, any variational state that minimizes the energy must be a ground-state. This wavefunction will be reformulated into a tensor network in the next section to be feed into a numerical scheme called corner transfer matrix renormalization group (CTMRG) for optimizing infinite tensor networks such as this. Before that, we will further motivate this variational ansatz with some theoretical results. Note that

$$|\alpha\rangle := \prod_p (1 + \alpha Z_p)|0\rangle$$

is the mean-field approximation of the perturbed ground-state. To justify this, note that $|\alpha = 0\rangle$ is the vacuum state, which is the ground-state in the large string-tension limit, and that

$$|\alpha = 1\rangle = \prod_p 2B_p|0\rangle$$

is proportional to the unique non-trivial ground-state of a string-net model on an open disk exhibiting a topological order, as determined in [17] that $\prod_p B_p$ acting on the vacuum state produces the equal superposition of all string-net configurations. This establishes $|\alpha\rangle$ as a linear interpolation of the two states with different topological order, and the decomposition

$$\langle\alpha|\prod_p B_p|\alpha\rangle = \prod_p \langle\alpha|B_p|\alpha\rangle \, ,$$

devised in [4], further justified the state as the mean-field approximation, in that the fluxes (measured by B_p) in the state is indepedent from each other.

3.1.1 Topological order parameter

The alternative method, to be elaborated in the discussion section, is to not assume any functional form of the ground-state wavefunction, and instead have the variational state be randomly initiated as a huge tensor [24, 25], whose size depend on the bond dimension of some tensor network to be introduced in the next section. This method, though exact, do not come with a way to measure the topological order parameter for judging whether or not the phase transition have taken place. Therefore, in general models this method is only used for brenchmarking against other parametric method in terms of the exact energy values it produces, say, for determining if convergence is sufficient at some bond dimensions.

Our method provides a way to determine the topological order for any intermediate ground-states between the small and large string-tension limits, by looking at α^* as a function of θ . The following results are obtained.

Theorem. *The non-local operator $\prod_p B_p$ is a topological order parameter.*

Proof. Denote the unique ground-state with a topological order of the string-net model as $|GS\rangle$. In the topologically orderred phase

$$\prod_p B_p|GS\rangle = \prod_p B_p \prod_p B_p|0\rangle = \prod_p B_p|0\rangle = |GS\rangle \, ,$$

and so $\prod_p B_p$ has a non-zero expectation in this phase. Next, in the trivial phase for which $|0\rangle$ is the ground-state,

$$\langle 0|\prod_p B_p|0\rangle = \langle 0|GS\rangle = 0 \, .$$

The last equality holds because $|GS\rangle$ is the equal superposition of infinitely many string-net configurations on the infinite honeycomb lattice, and that the vacuum $|0\rangle$ is only one of the valid string-net configurations. Recall that the Hilbert space is defined such that the string-net configurations forms an orthonormal basis, overlap of the two states must tends to zero in the thermodynamic limit. So, $\prod_p B_p$ has an expectation of zero outside the orderred phase. Finally, it commutes with the string-net Hamiltonian as all B_p commute.

When $\theta \neq 0$, the new ground-state is obtained from $|GS\rangle$ by applying a sum of local operators, and the support of these local operators only scales exponentially with the linear size [26, 27]. Denote the new ground-state at some fixed $\theta \neq 0$ as $|GS'\rangle = V|GS\rangle$ where V is the sum of local perturbations. Then

$$\langle GS'|\prod_p B_p|GS'\rangle = \langle GS|V^\dagger \prod_p B_p V|GS\rangle$$

shows that the expectation value of $\prod_p B_p$ in the perturbed state is the same as computing the expectation for a decorated operator $V^\dagger \prod_p B_p V$ on the fixed-point ground-state. Expanding $\prod_p B_p$ as a sum of deconfined string-operators, whose expectations scale as the perimeter-law of linear size [28], it is assumed that perturbing these string-operators with the local operators will not change whether the expectation evaluated is one or zero at the thermodynamic limit. □

In spontaneous symmetry-breaking (SSB) of a group symmetry into one of its subgroup, the expectation of the local order parameter, as a function of the parameter that drives the phase transtition, has the property that its continuity or discontinuity reflects whether or not the phase transition is continuous. This property is nonetheless loss for our topological order parameter. To gauge the continuity of the topological phase transition, we point to results relating the continuity of $\alpha^*(\theta)$ to that of the energy density $e_{plaq}(\theta)$ per plaquette. Using the closed-form expression for energy in terms of α in [4], one sees that any discontinuity in $e_{plaq}(\theta)$ implies the discontinuity of $\alpha^*(\theta)$ at that θ. The reverse direction of the implication holds for some neighborhood of θ for all values of θ.

3.2   Tensor network representation of the charge-free string-net model with string-tension

In [2], the term $\prod_p e^{-\eta B_p}$ is dropped without sufficient justification. Their ansatz

$$|\alpha, \beta, 0\rangle = \mathcal{N} \prod_l e^{\beta L_l} \prod_p (1 + \alpha Z_p)|0\rangle \ ,$$

however, still contain the mean-field approximation [4] as a special case when $\beta = 0$, and so it is at least as accurate as the mean-field ansatz. Still, the implication of their result is limited, since dropping the above term results in an ansatz that is, like the mean-field ansatz, only perturbatively exact to the zeroth order - while the mean-field ansatz has already been worked out analytically. Indeed, [2] produced the same prediction as the mean-field ansatz: a continuous phase transition for Z_2 fusion rules, and a discontinuous phase transition for Fibonacci fusion rules. The disagreement between the mean-field closed-form solution and the earlier result with exact diagonalization [1] remains unsettled.

In this work, it is shown that the term $B = \prod_p e^{-\eta B_p}$ can be incorporated without increasing the computational complexity of the tensor network representation, allowing all first corrections to be accounted for. The following change of variable shows that a B-perturbed ground-state of the theory, denoted by the collection quantum dimensions $(d_s)_s$, can be rewritten as the unperturbed (by B) ground-state for some rescaled theory $(\widetilde{d_s})_s$ up to a

scalar multiple :

$$
\begin{aligned}
|\alpha,\beta,\eta\rangle &= \mathcal{N}\prod_l e^{\beta L_l}\prod_p e^{-\eta B_p}\prod_p(1+\alpha Z_p)|0\rangle \\
&= \mathcal{N}\prod_l e^{\beta L_l}\prod_p\left[1+(-\eta+\tfrac{1}{2}\eta^2-\dots)B_p\right]\prod_p(1+\alpha Z_p)|0\rangle \\
&= \mathcal{N}\prod_l e^{\beta L_l}\prod_p\left[1+(e^{-\eta}-1)B_p\right]\prod_p(1-\alpha+2\alpha B_p)|0\rangle \\
&= \mathcal{N}\prod_l e^{\beta L_l}\prod_p\left\{1-\alpha+\left[(1+\alpha)e^{-\eta}+\alpha-1\right]B_p\right\}|0\rangle \\
&= \mathcal{N}\frac{1}{D^{2N_{\mathrm{plaq}}}}\prod_l e^{\beta L_l}\prod_p\left[(1-\alpha)D^2+A(\alpha,\eta)\sum_s d_s B_p^s\right]|0\rangle \\
&= \frac{1}{D^{2N_{\mathrm{plaq}}}}\frac{\mathcal{N}}{\left[(1-\alpha)D^2+A(\alpha,\eta)\right]^{N_{\mathrm{plaq}}}}\prod_l e^{\beta L_l}\prod_p(1+\gamma\sum_{s\neq0}d_s B_p^s)|0\rangle \\
&= \widetilde{\mathcal{N}}\prod_l e^{\beta L_l}\prod_p\widetilde{B_p}|0\rangle
\end{aligned}
$$

where N_{plaq} is the total number of plaquette, and the following substitutions and defined

$$
\begin{aligned}
A(\alpha,\eta) &:= (1+\alpha)e^{-\eta}+\alpha-1 \\
\gamma &:= \frac{A(\alpha,\eta)}{(1-\alpha)D^2+A(\alpha,\eta)} \\
\widetilde{\mathcal{N}} &:= \frac{\mathcal{N}}{\left[(1-\alpha)D^2+A(\alpha,\eta)\right]^{N_{\mathrm{plaq}}}} \\
\widetilde{B_p} &:= \sum_s\frac{\widetilde{d_s}}{D^2}B_p^s\ ,\ \text{with } \widetilde{d_s}:=\begin{cases}\gamma d_s\ ,\ s\neq0 \\ d_s\ ,\ s=0\end{cases}
\end{aligned}
$$

We are now in position to build the variational infinite PEPS.

3.2.1   Ground-state wavefunction

Following [21],

where the orange loop in plaquette p is of type μ_p, and this loop configuration $\mu=\{\mu_p\}_p$ is summed over. That is, the tensor contraction is computed at every fixed loop configuration,

and then the result is summed up. The unitcell in the tensor diagram is

and it will be used as the site tensor on a square lattice.

Across each link,

and factor $\sqrt{\frac{d_c}{d_a d_b}}$ is shared between the two neighboring site tensors. Each tensor absorb a square root of this factor such that the tensor contraction on this link will recovery the factor.

The tensor diagom at each vertex is, up to a π-rotation,

Let G^{abc}_{def} be the symmetrization of F^{bfa}_{cda} and defined by

$$G^{abc}_{def} = F^{bfa}_{cda} \cdot \frac{1}{\sqrt{d_a d_d}} \ ,$$

so that the factor derived on a vertex becomes

$$G^{abc}_{def} \cdot \sqrt{d_f d_e d_d}$$

Finally, each plaquette p comes with a factor of $\widetilde{d_{\mu_p}}$ where μ_p is the string-type inside p for that loop-configuration. This factor is splitted among the six neighboring site tensors, and so each tensor receives a sixth-root of $\widetilde{d_{\mu_p}}$ from three different plaquettes p.

Putting everything together, the summand of $\sum_\mu$ is decomposed into a tensor contraction of the following site tensor (up to a π-rotation)

$$= \delta_{aa'}\delta_{bb'}\delta_{cc'}\delta_{dd'}\delta_{ee'}\delta_{ff'}(\widetilde{d_d}\widetilde{d_e}\widetilde{d_f})^{\frac{1}{6}}(d_a d_b d_c)^{\frac{1}{4}}G^{abc}_{def}$$

where the original physical indices a, b, c are pulled through and out of the sites using delta functions, and therefore, the physical indices a', b', c' now point out from the vertices.

13

Relation to projected entangled-simplex state An alterative is to define entanglement simplex tensors on the vertices, and insert site tensors at the links [21], resulting in a projected entangled-simplex state where physical degrees of freedom are entangled in groups of three rather than two.
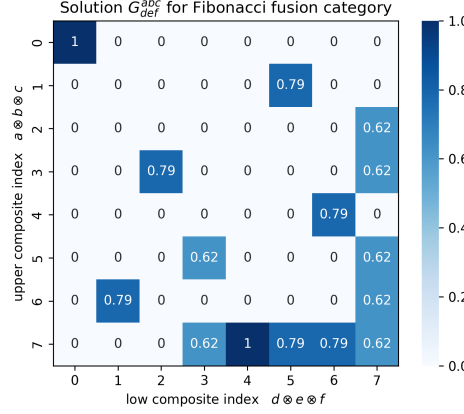

Figure 1: Symmetrization G^{abc}_{def} of associator for Fibonacci fusion category, represented by flattening it into a matrix.

3.2.2 Action of Hamiltonian on the entanglement level

Rewrite the Hamiltonian into local terms $H = \sum_p H_p$,

$$H_p = -\frac{sin\theta}{2} \sum_{l \in \partial p} L_l - cos\theta B_p$$

The Hamiltonian consist of a 12-site interaction, and writing it as a matrix acting on the 12-site local Hilbert space will cause memory error to the computer. Therefore, we will pull back the B_p operator through the PEPS-map onto the virtual level, and then decomposite it into a matrix product operator acting on the entanglement degrees of freedom. In general, this is possible when the PEPS constructed is an injective linear map [16].

For the plaquette operator B_q, swapping out the virtual index μ_p gives

$$\begin{aligned}
B_q|\alpha, \beta, \eta\rangle &= \sum_s \frac{d_q}{D^2} B^s_q \cdot \widetilde{N} \prod_l e^{\beta L_l} \sum_\mu \prod_p \frac{\widetilde{d}_{\mu_p}}{D^2} B^{\mu_p}_p |0\rangle \\
&= \sum_{s\mu} \frac{d_s}{D^2} \cdot \widetilde{N} \prod_l e^{\beta L_l} \left(\prod_p \frac{\widetilde{d}_{\mu_p}}{D^2}\right) \left(\prod_{p \neq q} B^{\mu_p}_p\right) \left(\sum_{\widetilde{\mu}_q} N^{\widetilde{\mu}_q}_{s\mu_q} B^{\widetilde{\mu}_q}_q\right)|0\rangle \;, \text{ by fusion algebra,} \\
&= \sum_{s\mu\widetilde{\mu}_q} \frac{1}{D^2} \frac{d_s \widetilde{d}_{\widetilde{\mu}_q}}{\widetilde{d}_{\mu_q}} N^{\mu_q}_{s\widetilde{\mu}_q} \cdot \widetilde{N} \prod_l e^{\beta L_l} \prod_p \frac{\widetilde{d}_{\mu_p}}{D^2} B^{\mu_p}_p |0\rangle \quad , \text{ by swapping } \mu_q \leftrightarrow \widetilde{\mu}_q \;, \\
&= \frac{1}{D^2} \sum_{ab} N^{\mu_q}_{ab} \frac{d_a \widetilde{d}_b}{\widetilde{d}_{\mu_q}} |\alpha, \beta, \eta\rangle
\end{aligned}$$

14

By writing the action of B_p depend solely on the virtual index μ_p, and it is scalar multiplication by

$$\Phi(\mu_p) = \frac{1}{D^2} \sum_{ab} N_{ab}^{\mu_q} \frac{d_a \widetilde{d}_b}{\widetilde{d}_{\mu_q}}$$

3.2.3 Corner transfer matrix renormalization group

Infinite PEPS is represented by a bulk tensor T with its four virtual bond connected to a boundary MPS. The boundary MPS acts as the infinitely large environment, and is obtained by solving the renormalization group (RG) fixed point equation numerically. These methods include for example the power method for finding eigenvalues and the corner transfer matrix renormalization group (CTMRG) [29] used in this work. The bulk tensor is chosen to be the abovementioned unitcell. It has a π-rotational symmetry, and this is exploited to greatly simply the boundary MPS implementation.

4 Result & discussion

The first stage of implementing the above scheme is to run a simulation while fixing $\beta = 0$ and η. This is because the model is should then reproduce the mean-field result in [4], which is exact and acts a valid brenchmark. This stage is also used to find the boundary MPS bond dimension needed to give good results, since the non-parametric tensor network cannot be applied for this model.

Figure 2 shows that mean-field variational energy landscape obtained by SNST with the Tambara-Yamgami category for $\mathbb{Z}_3$ (TY_3) as the input UFC.
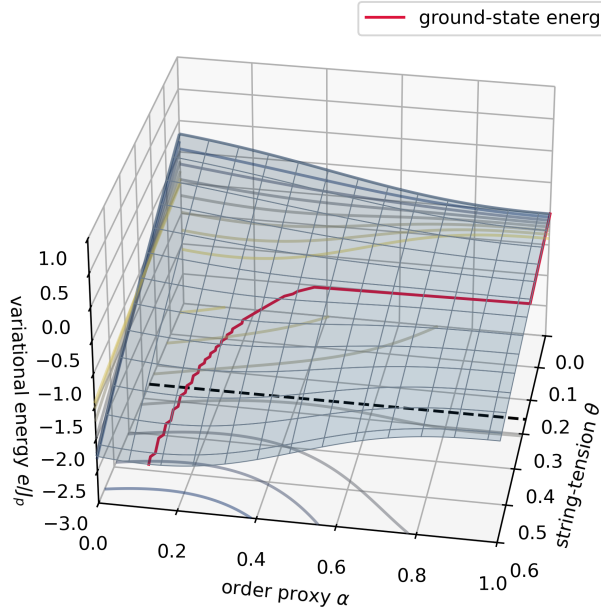

Figure 2: Mean-field tensor network ansatz applied on TY3 string-net model. The dotted line marks the predicted phase transition point θ_c.
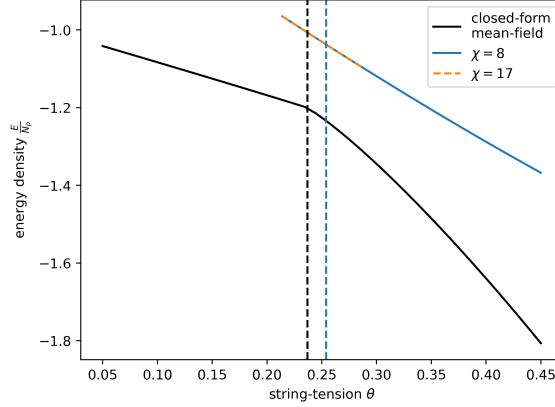
Figure 3: Mean-field tensor network ansatz applied to perturbed the double $\mathbb{Z}_2$ topological order of string-net model.The black and blue dotted lines mark the phase transition points predicted in reference [30] with mean-field and one-sided first order tensor network ansatz respectively.

4.1 Failure in convergence

The simulation for TY_3 fails under memory error even when the smallest possible boundary MPS bond dimension (also called environental bond dimension) of 2 if used. The CTMRG is ran on the STSN with Fibonacci fusion rules for environemental bond dimension 8 and 17, and the result is shown in figure 3.

As can be seen from figure 3, there are huge discrepancies from the analytic result. The environmental bond dimension used in [4] is, however, not mentioned in their paper. Still, from the fact that increasing the bond dimension from 8 to 17 does not change the prediction significantly, it can be implied that the currently environment bond dimension is far below what is needed.

4.2 Qualitative statement on the first-order correction

Interesting, we know the qualitative difference that the first-order correction will bring to the prediction of α.

First, notice that our model with η fixed at 0 reduces back to that used in [2]. Smoothly varying string tension will eventually see a jump (discontinuity) in the optimal value $\alpha*$ for parameter α from one to another value. Our new tensor network representation incorporates the extra perturbation parameter η for the ansatz to be exact up to first-order. This extra freedom means that the optimal value can move up along the level sets shown in figure 5. From the slope of the level sets, we see that implementing our model delays the phase transition to a larger critical string-tension value θ_c, because a decrease in α has the same effect on the resulting energy evaluation as some increase in η. Still, whether this postponement will close the discontinuity cannot be known without the numerics.
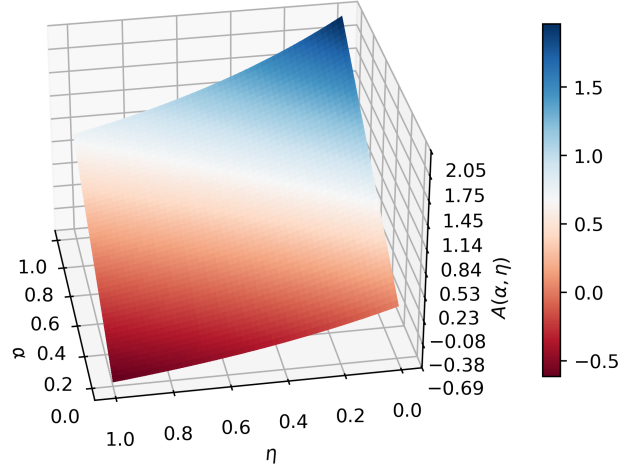
16

Figure 4: Function A used in the homogenization of the first-order ansatz.
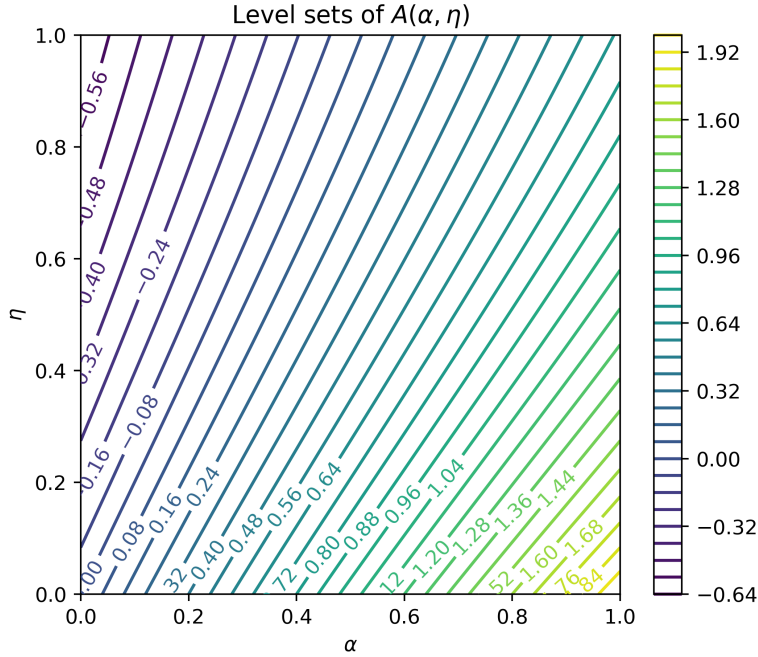

Figure 5: Level sets of A over the full range for the two variational parameters involved.

4.3 Comparison with the non-parametric variational tensor network method

For simpler systems, and "simple" means that they lack extended interaction terms like the 12-site interaction in string-net model, the non-parameteric variational tensor network method can be used [24, 25]. This general method does not assume any functional form for the ground-state wavefunction, and instead randomly initiate the variational state as a large tensor, whose size depend on the bond dimension. There are two limitations to this

non-parametric method that our method do not face. First, the non-parametric method, though produce an exact ground-state, do not come with ways of extracting information like the topological order. Second, the computer memory needed to implement this method on this model is impractically large, due to the 12-site interaction.

4.4 Future directions

A future direction for study is to run the simulation for larger environment bond dimension in the Fibonnaci fusion rules. However, it is apparant from the result with TY_3 that the choice of model may be wrong in the first place. The motivation to use the SNST is that it realizes a large class of topological orders, and so any numerical scheme developed on it will immediately works for studying all the achiral doubled topological order in 2+1d. The TY_3 UFC is, however, only two simple objects more than the Fibonacci UFC, and yet, the tensor network scheme was already pushed to its limit. It means that for the more general problem of topological phase transition, models without extended interaction terms are more promising directions numerically.

5 Acknowledgement

References

[1] Marc Daniel Schulz et al. "Topological Phase Transitions in the Golden String-Net Model". In: *Phys. Rev. Lett.* 110 (14 Apr. 2013), p. 147203. DOI: 10.1103/PhysRevLett.110.147203. URL: https://link.aps.org/doi/10.1103/PhysRevLett.110.147203.

[2] Alexis Schotte et al. "Tensor-network approach to phase transitions in string-net models". In: *Phys. Rev. B* 100 (24 Dec. 2019), p. 245125. DOI: 10.1103/PhysRevB.100.245125. URL: https://link.aps.org/doi/10.1103/PhysRevB.100.245125.

[3] Laurens Vanderstraeten et al. "Bridging Perturbative Expansions with Tensor Networks". In: *Phys. Rev. Lett.* 119 (7 Aug. 2017), p. 070401. DOI: 10.1103/PhysRevLett.119.070401. URL: https://link.aps.org/doi/10.1103/PhysRevLett.119.070401.

[4] Sébastien Dusuel and Julien Vidal. "Mean-field ansatz for topological phases with string tension". In: *Phys. Rev. B* 92 (12 Sept. 2015), p. 125150. DOI: 10.1103/PhysRevB.92.125150. URL: https://link.aps.org/doi/10.1103/PhysRevB.92.125150.

[5] Xie Chen, Zheng-Cheng Gu, and Xiao-Gang Wen. "Local unitary transformation, long-range quantum entanglement, wave function renormalization, and topological order". In: *Phys. Rev. B* 82 (15 Oct. 2010), p. 155138. DOI: 10.1103/PhysRevB.82.155138. URL: https://link.aps.org/doi/10.1103/PhysRevB.82.155138.

[6] P.W. Shor. "Fault-tolerant quantum computation". In: *Proceedings of 37th Conference on Foundations of Computer Science*. 1996, pp. 56–65. DOI: 10.1109/SFCS.1996.548464.

[7] T. I. Andersen et al. "Non-Abelian braiding of graph vertices in a superconducting processor". In: *Nature* 618.7964 (June 2023), pp. 264–269. ISSN: 1476-4687. DOI: 10.1038/s41586-023-05954-4. URL: https://doi.org/10.1038/s41586-023-05954-4.

[8] Mohsin Iqbal et al. "Non-Abelian topological order and anyons on a trapped-ion processor". In: *Nature* 626.7999 (Feb. 2024), pp. 505–511. ISSN: 1476-4687. DOI: 10.1038/s41586-023-06934-4. URL: https://doi.org/10.1038/s41586-023-06934-4.

[9] Shibo Xu et al. "Non-Abelian braiding of Fibonacci anyons with a superconducting processor". In: *Nature Physics* 20.9 (Sept. 2024), pp. 1469–1475. ISSN: 1745-2481. DOI: 10.1038/s41567-024-02529-6. URL: https://doi.org/10.1038/s41567-024-02529-6.

[10] Tomoyuki Morimae. "Quantum computational tensor network on string-net condensate". In: *Phys. Rev. A* 85 (6 June 2012), p. 062328. DOI: 10.1103/PhysRevA.85.062328. URL: https://link.aps.org/doi/10.1103/PhysRevA.85.062328.

[11] Zlatko K. Minev et al. "Realizing string-net condensation: Fibonacci anyon braiding for universal gates and sampling chromatic polynomials". In: (June 2024). arXiv: 2406.12820 [quant-ph].

[12] Brendan Pankovich. "The String-Net Surface Code: Quantum Circuits for Doubled Topological Phases". PhD thesis. Utah U. (main), Mar. 2019.

[13] L. LANDAU. "The Theory of Phase Transitions". In: *Nature* 138.3498 (Nov. 1936), pp. 840–841. ISSN: 1476-4687. DOI: 10.1038/138840a0. URL: https://doi.org/10.1038/138840a0.

[14] X. G. Wen and Q. Niu. "Ground-state degeneracy of the fractional quantum Hall states in the presence of a random potential and on high-genus Riemann surfaces". In: *Phys. Rev. B* 41 (13 May 1990), pp. 9377–9396. DOI: 10.1103/PhysRevB.41.9377. URL: https://link.aps.org/doi/10.1103/PhysRevB.41.9377.

[15] Wenjie Ji and Xiao-Gang Wen. "Categorical symmetry and noninvertible anomaly in symmetry-breaking and topological phase transitions". In: *Phys. Rev. Res.* 2 (3 Sept. 2020), p. 033417. DOI: 10.1103/PhysRevResearch.2.033417. URL: https://link.aps.org/doi/10.1103/PhysRevResearch.2.033417.

[16] N. Bultinck et al. "Anyons and matrix product operator algebras". In: *Annals of Physics* 378 (2017), pp. 183–233. ISSN: 0003-4916. DOI: https://doi.org/10.1016/j.aop.2017.01.004. URL: https://www.sciencedirect.com/science/article/pii/S0003491617300040.

[17] Chien-Hung Lin, Michael Levin, and Fiona Burnell. *Generalized string-net models: A thorough exposition*. Dec. 2020. DOI: 10.48550/arXiv.2012.14424.

[18] Anna Ritz-Zwilling et al. *Finite-temperature properties of string-net models*. June 2024. DOI: 10.48550/arXiv.2406.19713.

[19] André O. Soares, Anna Ritz-Zwilling, and Jean-Noël Fuchs. "Extended string-net models with all anyons at finite temperature". In: (Feb. 2025). arXiv: 2502.01454 [cond-mat.mes-hall].

[20] Matthew B. Hastings. "Topological Order at Nonzero Temperature". In: *Phys. Rev. Lett.* 107 (21 Nov. 2011), p. 210501. DOI: 10.1103/PhysRevLett.107.210501. URL: https://link.aps.org/doi/10.1103/PhysRevLett.107.210501.

[21] Oliver Buerschaper, Miguel Aguado, and Guifré Vidal. "Explicit tensor network representation for the ground states of string-net models". In: *Phys. Rev. B* 79 (8 Feb. 2009), p. 085119. DOI: 10.1103/PhysRevB.79.085119. URL: https://link.aps.org/doi/10.1103/PhysRevB.79.085119.

[22] Zheng-Cheng Gu et al. "Tensor-product representations for string-net condensed states". In: *Phys. Rev. B* 79 (8 Feb. 2009), p. 085118. DOI: 10.1103/PhysRevB.79.085118. URL: https://link.aps.org/doi/10.1103/PhysRevB.79.085118.

[23] J. Ignacio Cirac et al. "Matrix product states and projected entangled pair states: Concepts, symmetries, theorems". In: *Rev. Mod. Phys.* 93 (4 Dec. 2021), p. 045003. DOI: 10.1103/RevModPhys.93.045003. URL: https://link.aps.org/doi/10.1103/RevModPhys.93.045003.

[24] Laurens Vanderstraeten et al. "Variational methods for contracting projected entangled-pair states". In: *Phys. Rev. B* 105 (19 May 2022), p. 195140. DOI: 10.1103/PhysRevB.105.195140. URL: https://link.aps.org/doi/10.1103/PhysRevB.105.195140.

[25] Hai-Jun Liao et al. "Differentiable Programming Tensor Networks". In: *Phys. Rev. X* 9 (3 Sept. 2019), p. 031041. DOI: 10.1103/PhysRevX.9.031041. URL: https://link.aps.org/doi/10.1103/PhysRevX.9.031041.

[26] Sergey Bravyi, Matthew B. Hastings, and Spyridon Michalakis. "Topological quantum order: Stability under local perturbations". In: *Journal of Mathematical Physics* 51.9 (Sept. 2010), p. 093512. ISSN: 0022-2488. DOI: 10.1063/1.3490195. eprint: https://pubs.aip.org/aip/jmp/article-pdf/doi/10.1063/1.3490195/14759707/093512_1_online.pdf. URL: https://doi.org/10.1063/1.3490195.

[27] Sergey Bravyi and Matthew B. Hastings. "A Short Proof of Stability of Topological Order under Local Perturbations". In: *Communications in Mathematical Physics* 307.3 (Nov. 2011), pp. 609–627. ISSN: 1432-0916. DOI: 10.1007/s00220-011-1346-2. URL: https://doi.org/10.1007/s00220-011-1346-2.

[28] M. B. Hastings and Xiao-Gang Wen. "Quasiadiabatic continuation of quantum states: The stability of topological ground-state degeneracy and emergent gauge invariance". In: *Phys. Rev. B* 72 (4 July 2005), p. 045141. DOI: 10.1103/PhysRevB.72.045141. URL: https://link.aps.org/doi/10.1103/PhysRevB.72.045141.

[29] M. T. Fishman et al. "Faster methods for contracting infinite two-dimensional tensor networks". In: *Phys. Rev. B* 98 (23 Dec. 2018), p. 235148. DOI: 10.1103/PhysRevB.98.235148. URL: https://link.aps.org/doi/10.1103/PhysRevB.98.235148.

[30] Alexis Schotte et al. "Tensor-network approach to phase transitions in string-net models". In: *Phys. Rev. B* 100 (24 Dec. 2019), p. 245125. DOI: 10.1103/PhysRevB.100.245125. URL: https://link.aps.org/doi/10.1103/PhysRevB.100.245125.